Physics Letters B 736 (2014) 186–195

Contents lists available at ScienceDirect

Physics Letters B

www.elsevier.com/locate/physletb

Measurement of the *CP*-violating phase ϕ_s in $\overline{B}{}^0_s \to J/\psi\pi^+\pi^-$ decays

LHCb Collaboration

ARTICLE INFO

Article history:
Received 16 May 2014
Received in revised form 25 June 2014
Accepted 30 June 2014
Available online 3 July 2014
Editor: W.-D. Schlatter

ABSTRACT

The mixing-induced *CP*-violating phase ϕ_s in B^0_s and $\overline{B}{}^0_s$ decays is measured using the $J/\psi\pi^+\pi^-$ final state in data, taken from 3 fb^{-1} of integrated luminosity, collected with the LHCb detector in 7 and 8 TeV centre-of-mass pp collisions at the LHC. A time-dependent flavour-tagged amplitude analysis, allowing for direct *CP* violation, yields a value for the phase $\phi_s = 70 \pm 68 \pm 8$ mrad. This result is consistent with the Standard Model expectation and previous measurements.

1. Introduction

One of the most sensitive ways of detecting the presence of heretofore unseen particles or forces is through the observation of effects they may have on *CP*-violating decays of neutral B mesons [1]. Measurements of *CP* violation through the interference of B^0_s mixing and decay amplitudes are particularly sensitive because the Standard Model (SM) prediction of the *CP*-violating phase is very small and accurate in quark level $b \to c\bar{c}s$ transitions, with $\phi_s^{\rm SM} \equiv -2\arg(-\frac{V_{ts}V_{tb}^*}{V_{cs}V_{cb}^*}) = -36.3^{+1.6}_{-1.5}$ mrad, ignoring subleading corrections from Penguin amplitudes [2]. Initial measurements of ϕ_s at the Tevatron indicated possible large values inconsistent with the SM expectation [3], while LHCb measurements using both $\overset{(-)}{B}{}^0_s \to J/\psi\phi$ and $\overset{(-)}{B}{}^0_s \to J/\psi\pi^+\pi^-$ decays from 1 fb^{-1} of integrated luminosity were consistent with the SM value [4,5], as were more recent results from CDF [6], and ATLAS [7].

In this Letter, we present a new measurement of ϕ_s in $\overset{(-)}{B}{}^0_s \to J/\psi\pi^+\pi^-$ decays using data taken from an integrated luminosity of 3 fb^{-1}, obtained from pp collisions at the LHC. One-third of the data was collected at a centre-of-mass energy of 7 TeV, and the remainder at 8 TeV. In the previous study we used the result of our amplitude analysis [8], which showed that the *CP*-odd component of the decay was larger than 97.7% at 95% confidence level (CL). Here we perform a more sophisticated amplitude analysis [9], which uses an additional angular variable, and thereby directly determines the *CP*-odd and *CP*-even components. Previously it was found that five interfering $\pi^+\pi^-$ states required to describe the decay are: $f_0(980)$, $f_0(1500)$, $f_0(1790)$, $f_2(1270)$, and $f_2'(1525)$ [10]. In the same analysis, an alternative model including these states and a nonresonant $J/\psi\pi^+\pi^-$ component was also found to provide a good description of the data; the limit on the *CP*-even component is unchanged. The $J/\psi f_0(980)$ final state was suggested as being a useful final state for measuring ϕ_s as it is a *CP*-eigenstate [11] and inspired these studies. Subsequently, it was suggested that the $f_0(980)$ resonance might be formed of tetraquarks [12], and could then provide an additional SM contribution to ϕ_s beyond that originally expected. Studies of $\overline{B}_0 \to J/\psi\pi^+\pi^-$ decays [13] indicate that the light scalar mesons are familiar $q\bar{q}$ states [14], so this concern has been ameliorated.

The method used here allows the measurement of the *CP*-violating phase ϕ_s, without any assumption on the *CP* content, by measuring simultaneously the *CP*-even and *CP*-odd decay amplitudes and ϕ_s.

2. Decay rates for $\overline{B}{}^0_s \to J/\psi h^+h^-$

The time dependent formalism for decays of neutral B mesons to a J/ψ meson, that subsequently decays into a $\mu^+\mu^-$ pair, and two pseudo-scalar particles h^+h^- is derived in Ref. [9]. The differential decay rates for $\overset{(-)}{B}{}^0_s \to J/\psi h^+h^-$, allowing for possible direct *CP* violation, can be written in terms of the decay time t, and the decay amplitudes $\mathcal{A}$ and $\overline{\mathcal{A}}$ as [15]

$$\begin{aligned}\Gamma(t) = \mathcal{N}e^{-\Gamma_s t}\Bigg\{&\frac{|\mathcal{A}|^2+|\overline{\mathcal{A}}|^2}{2}\cosh\frac{\Delta\Gamma_s t}{2}\\ &+\frac{|\mathcal{A}|^2-|\overline{\mathcal{A}}|^2}{2}\cos(\Delta m_s t) - \mathcal{R}e\big(\mathcal{A}^*\overline{\mathcal{A}}\big)\sinh\frac{\Delta\Gamma_s t}{2}\\ &-\mathcal{I}m\big(\mathcal{A}^*\overline{\mathcal{A}}\big)\sin(\Delta m_s t)\Bigg\},\end{aligned} \tag{1}$$

$$\begin{aligned}\overline{\Gamma}(t) = \left|\frac{p}{q}\right|^2\mathcal{N}e^{-\Gamma_s t}\Bigg\{&\frac{|\mathcal{A}|^2+|\overline{\mathcal{A}}|^2}{2}\cosh\frac{\Delta\Gamma_s t}{2}\\ &-\frac{|\mathcal{A}|^2-|\overline{\mathcal{A}}|^2}{2}\cos(\Delta m_s t) - \mathcal{R}e\big(\mathcal{A}^*\overline{\mathcal{A}}\big)\sinh\frac{\Delta\Gamma_s t}{2}\\ &+\mathcal{I}m\big(\mathcal{A}^*\overline{\mathcal{A}}\big)\sin(\Delta m_s t)\Bigg\},\end{aligned} \tag{2}$$

http://dx.doi.org/10.1016/j.physletb.2014.06.079

where $\Delta\Gamma_s \equiv \Gamma_L - \Gamma_H$ is the decay width difference between the light and the heavy mass eigenstates, $\Delta m_s \equiv m_H - m_L$ is the mass difference, $\Gamma_s \equiv (\Gamma_L + \Gamma_H)/2$ is the average width, and $\mathcal{N}$ is a constant. The complex parameters q and p are used to relate the mixing between the mass and flavour eigenstates. The decay amplitudes are defined as $\mathcal{A} \equiv A_f$ and $\overline{\mathcal{A}} \equiv \frac{q}{p}\overline{A}_f$, where A_f ($\overline{A}_f$) is the total amplitude of B_s^0 ($\overline{B}_s^0$) $\to J/\psi h^+h^-$ decays at time $t = 0$.

The total amplitude A_f ($\overline{A}_f$) is taken to be the sum over individual $\pi^+\pi^-$ resonant transversity amplitudes [16], and possibly one nonresonant amplitude, labelled as A_i ($\overline{A}_i$). By introducing the parameter $\lambda_i \equiv \frac{q}{p}\frac{\overline{A}_i}{A_i}$, relating CP violation in the interference between mixing and decay associated with the state i, the amplitudes $\mathcal{A}$ and $\overline{\mathcal{A}}$ can be further expressed as the sums of the individual $\overset{(-)}{B}{}_s^0$ amplitudes, $\mathcal{A} = \sum A_i$ and $\overline{\mathcal{A}} = \sum \lambda_i A_i$.

For J/ψ decays to $\mu^+\mu^-$ final states, these amplitudes are themselves functions of four variables: the $\pi^+\pi^-$ invariant mass $m_{hh} = m(\pi^+\pi^-)$, and the three angles Ω, defined in the helicity basis. These consist of the angle between the μ^+ direction in the J/ψ rest frame with respect to the J/ψ direction in the $\overset{(-)}{B}{}_s^0$ rest frame $\theta_{J/\psi}$, the angle between the h^+ direction in the h^+h^- rest frame with respect to the h^+h^- direction in the B_s^0 rest frame θ_{hh}, and the angle between the J/ψ and h^+h^- decay planes in the $\overline{B}_s^0$ rest frame χ [4,9].

Assuming that any possible CP violation in the decay is the same for all amplitudes, $\lambda \equiv \eta_i\lambda_i$ is common for all amplitudes, where η_i is the CP eigenvalue of the transversity state i. The CP-violating phase ϕ_s is defined by $\phi_s \equiv -\arg(\lambda)$ [4], and appears in the term containing $\mathcal{A}^*\overline{\mathcal{A}}$. The explicit forms of $|\overset{(-)}{\mathcal{A}}(m_{hh}, \Omega)|^2$ and $\mathcal{A}^*(m_{hh}, \Omega)\overline{\mathcal{A}}(m_{hh}, \Omega)$ in Eqs. (1) and (2) as functions of m_{hh} and Ω are given in Ref. [9].

The factor $|p/q|^2$ is related to the flavour-specific CP-violating asymmetry $a_{\rm sl}^s$ as

$$a_{\rm sl}^s \equiv \frac{|p/q|^2 - |q/p|^2}{|p/q|^2 + |q/p|^2} \approx |p/q|^2 - 1. \tag{3}$$

LHCb measured $a_{\rm sl}^s = (-0.06 \pm 0.50 \pm 0.36)\%$ [17], corresponding to $|p/q|^2 = 0.9994 \pm 0.0062$. Thus, we take $|p/q|^2 = 1$ for what follows.

3. The LHCb detector and event selection

The LHCb detector [18] is a single-arm forward spectrometer covering the pseudorapidity range $2 < \eta < 5$, designed for the study of particles containing b or c quarks. The detector includes a high-precision tracking system consisting of a silicon-strip vertex detector surrounding the pp interaction region, a large-area silicon-strip detector located upstream of a dipole magnet with a bending power of about 4 Tm, and three stations of silicon-strip detectors and straw drift tubes placed downstream. The combined tracking system provides a momentum measurement[1] with relative uncertainty that varies from 0.4% at 5 GeV to 0.6% at 100 GeV, and impact parameter resolution of 20 μm for tracks with large transverse momentum (p_T). Different types of charged hadrons are distinguished by information from two ring-imaging Cherenkov detectors. Photon, electron and hadron candidates are identified by a calorimeter system consisting of scintillating-pad and preshower detectors, an electromagnetic calorimeter and a hadronic calorimeter. The trigger consists of a hardware stage, based on information from the calorimeter and muon systems, followed by a software stage, which applies a full event reconstruction. Events selected for this analysis are triggered by a $J/\psi \to \mu^+\mu^-$ decay, where the J/ψ is required at the software level to be consistent with coming from the decay of a b hadron by use of either impact parameter requirements on the muons or detachment of the reconstructed J/ψ decay position from the associated primary vertex.

[1] We use units where $\hbar = c = 1$.

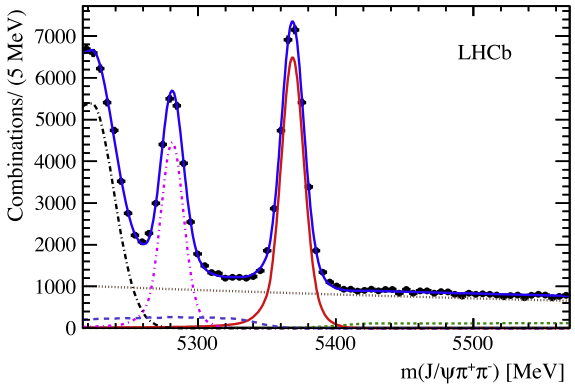

Fig. 1. Invariant mass of $J/\psi\pi^+\pi^-$ combinations. The data are fitted with double Crystal Ball signal functions and several background functions. The (red) solid line shows the $\overset{(-)}{B}{}_s^0$ signal, the (brown) dotted line shows the exponential combinatorial background, the (green) short-dashed line shows the $B^\mp$ background, the (magenta) dot-dashed line shows the $\overset{(-)}{B}{}^0$ signal, the (light blue) dashed line is the sum of $\overset{(-)}{B}{}_s^0 \to J/\psi\eta'$, $\overset{(-)}{B}{}_s^0 \to J/\psi\phi$, $\phi \to \pi^+\pi^-\pi^0$ backgrounds, and the $\Lambda_b^0 \to J/\psi K^- p$ plus $\overline{\Lambda}_b^0 \to J/\psi K^+\overline{p}$ reflections, the (black) dot-dashed line is the $\overset{(-)}{B}{}^0 \to J/\psi K^\mp\pi^\pm$ reflection and the (blue) solid line is the total. (The reader is referred to the web version of this article to see the figure in color.)

A $\overset{(-)}{B}{}_s^0 \to J/\psi\pi^+\pi^-$ candidate is reconstructed by combining a $J/\psi \to \mu^+\mu^-$ candidate with two pions of opposite charge. The like-sign combinations $J/\psi\pi^\pm\pi^\pm$ are also reconstructed for background studies. Events are selected using a multivariate method that optimizes the ratio of signal squared to background events. The event selection is described in detail in the time-integrated amplitude analysis [10]. The invariant mass distribution of $J/\psi\pi^+\pi^-$ combinations satisfying the event selection is shown in Fig. 1. Only the candidates within ±20 MeV of the $\overline{B}_s^0$ mass peak are retained for the ϕ_s measurement; there are $27\,100 \pm 200$ signal events with a purity of 79.6%. The integrated distributions of the four variables discussed above are shown in Fig. 2.

Samples of simulated events are used to characterize signal and backgrounds. In the simulation, pp collisions are generated using Pythia [19] with a specific LHCb configuration [20]. Decays of hadronic particles are described by EvtGen [21], in which final state radiation is generated using Photos [22]. The interaction of the generated particles with the detector and its response are implemented using the Geant4 toolkit [23], as described in Ref. [24].

4. Likelihood construction

We perform an unbinned maximum likelihood fit to the $J/\psi\pi^+\pi^-$ invariant mass m, the decay time t, m_{hh}, and the three helicity angles Ω, along with information on the initial flavour of the decaying hadron, *i.e.* whether it was produced as a B_s^0 or a $\overline{B}_s^0$ meson. The probability density function (PDF) used in the fit consists of signal and background components that include detector resolution and acceptance effects. The PDFs are factorized into separate components for the $\overline{B}_s^0$ mass and for the remaining observables.

The signal $\overset{(-)}{B}{}_s^0$ mass distribution is described by a double Crystal Ball function [25]. The background consists of a combinatorial component whose mass distribution is modelled by an exponen-

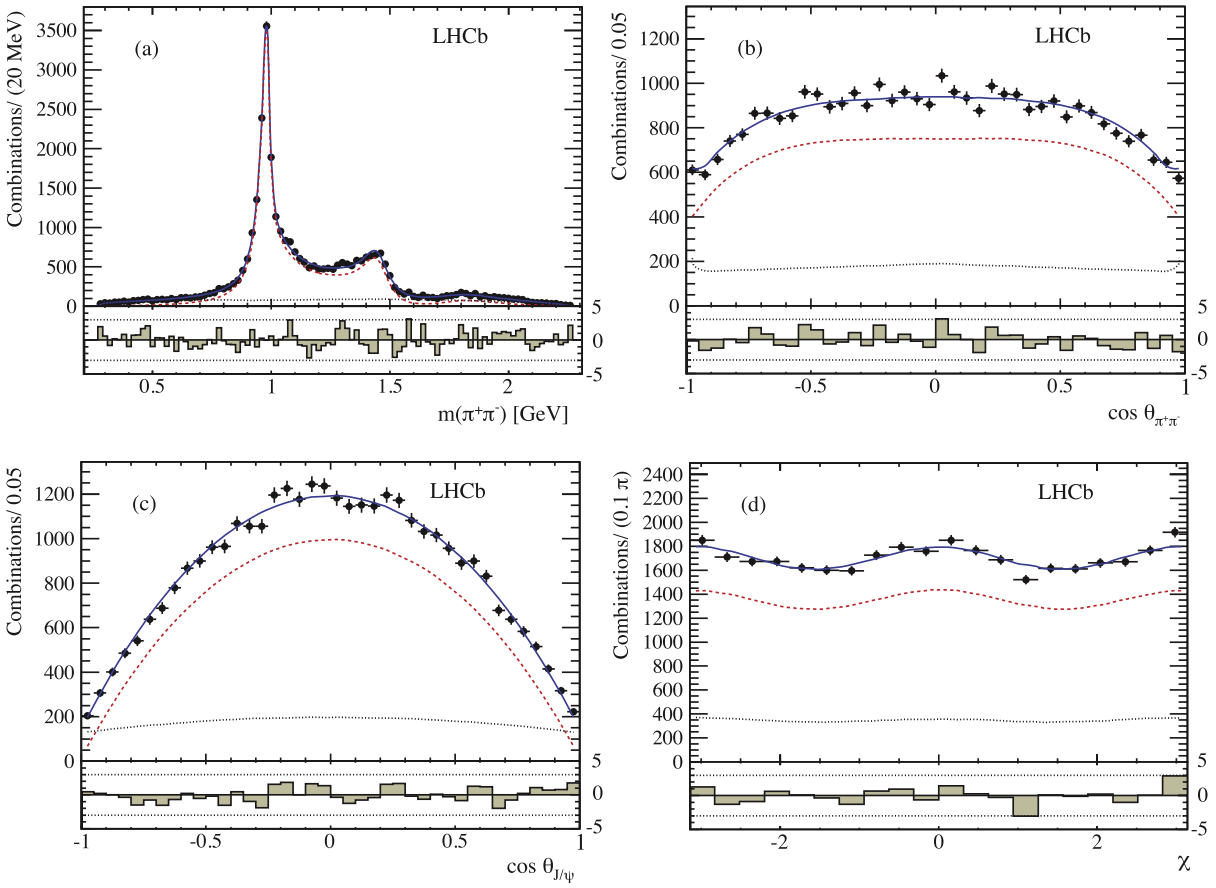

Fig. 2. Projections of (a) $m(\pi^+\pi^-)$, (b) $\cos\theta_{\pi\pi}$, (c) $\cos\theta_{J/\psi}$ and (d) χ [10]. The points with error bars are data, the signal fits are shown with (red) dashed lines, the background with a (black) dotted lines, and the (blue) solid lines represent the total fits. The difference between the data and the fits divided by the uncertainty on the data is shown below. (The reader is referred to the web version of this article to see the figure in color.)

tial function, a 2.3% contribution from the sum of $\overset{(-)}{B}{}^0_s \to J/\psi\eta'$ and $\overset{(-)}{B}{}^0_s \to J/\psi\phi$, with $\phi \to \pi^+\pi^-\pi^0$, and 2.0% from $B^\mp \to J/\psi K^\mp + J/\psi\pi^\mp$ decays, both of which produce tails in the $\overset{(-)}{B}{}^0_s$ signal region. The latter two background mass shapes are obtained from simulation. The parameters of the signal and the combinatorial background are obtained from a fit to the $\overset{(-)}{B}{}^0_s$ mass distribution in an extended region (see Fig. 1) and are subsequently fixed for use in the ϕ_s fit.

As can be seen from Eqs. (1) and (2), knowledge of the $\overset{(-)}{B}{}^0_s$ flavour at production greatly enhances the sensitivity. The process of determining the initial flavour is called "tagging". We use both opposite-side [26] and same-side tagging information [4,27]. The opposite-side (OS) tag identifies the flavour of another b hadron in the event using information from the charges of leptons and kaons from its decay, or the charge of another detached vertex. The same-side kaon (SSK) tagger utilizes the hadronization process, where the fragmentation of a b ($\bar{b}$) quark into $\overline{B}{}^0_s$ (B^0_s) meson can lead to an extra s ($\bar{s}$) quark being available to form a hadron, often leading to a K^- (K^+) meson. This kaon is correlated to the signal $\overset{(-)}{B}{}^0_s$ in phase space, and the sign of its charge identifies the initial flavour [27]. A wrong-tag probability η is estimated event-by-event, based on the output of a neural network trained on simulations. It is calibrated with data using flavour-specific decay modes in order to predict the true wrong-tag probability of the event $\overset{(-)}{\omega}(\eta)$ for an initial flavour $\overset{(-)}{B}{}^0_s$ meson, which has a linear dependence on η. The calibration is performed separately for the OS and the SSK taggers. Several modes are used for OS tagging including $B^\mp \to J/\psi K^\mp$, $B^\mp \to \overset{(-)}{D}{}^0\pi^\mp$, and fitting the oscillations in $\overset{(-)}{B}{}^0 \to J/\psi\overset{(-)}{K}{}^{*0}$ and $\overset{(-)}{B}{}^0 \to D^{*\pm}\mu^\mp\overset{(-)}{\nu}$ decays. SSK tags are calibrated by fitting the oscillations in $\overset{(-)}{B}{}^0_s \to D^\pm_s\pi^\mp$ decays. When events are tagged by both the OS and the SSK algorithms, a combined tag decision and wrong-tag probability are given by the algorithm defined in Ref. [26] and extended to include SSK tags. This combined algorithm is implemented in the overall fit. The overall effective tagging power obtained is characterized by $\varepsilon_{\rm tag}D^2 = (3.89\pm0.25)\%$, where $D \equiv (1-2\omega_{\rm avg})$ is the dilution, $\omega_{\rm avg}$ is the average wrong-tag probability, and $\varepsilon_{\rm tag} = (68.68\pm0.33)\%$ is the signal tagging efficiency. The overall tagging power is improved by about 60% with respect to the previous analysis [5] mainly due to the inclusion of the SSK tagger, which has an tagging power about 40% better than that described in Ref. [4], due to the use of a neural-network based selection. In addition, the OS algorithms discussed in Ref. [26] have been re-optimized using the full available dataset.

The theoretical signal function including flavour tagging is

$$R(\hat{t}, m_{hh}, \Omega, \mathrm{q}|\eta) = \frac{1}{1+|\mathrm{q}|}\Big[\big[1+\mathrm{q}\big(1-2\omega(\eta)\big)\big]\Gamma(\hat{t}, m_{hh}, \Omega) + \big[1-\mathrm{q}\big(1-2\bar{\omega}(\eta)\big)\big]\bar{\Gamma}(\hat{t}, m_{hh}, \Omega)\Big], \quad (4)$$

where $\hat{t}$ is the true decay time, and $\overset{(-)}{\Gamma}$ is defined in Eqs. (1) and (2). The flavour tag q takes values of -1, 1, 0, if the signal meson is tagged as $\overline{B}{}^0_s$, B^0_s, or untagged, respectively.

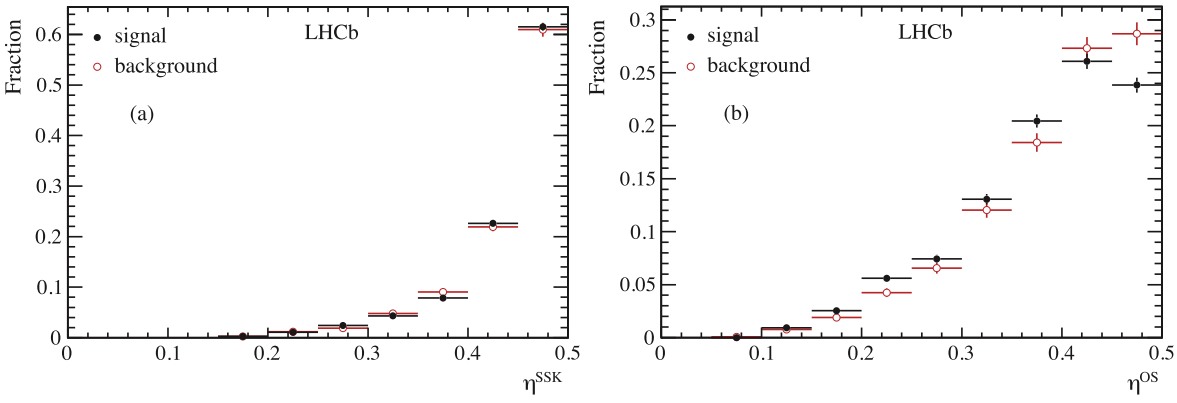

Fig. 3. Estimated fractions of mistag probabilities from (a) the SSK tagger, η^{SSK}, and (b) the OS tagger, η^{OS}.

The signal function is further modified to take into account the decay time resolution and the acceptance effects on all the fit variables

$$F^{sig}(t, m_{hh}, \Omega, \mathfrak{q}|\eta, \delta_t) = R(\hat{t}, m_{hh}, \Omega, \mathfrak{q}|\eta) \otimes T(t-\hat{t}|\delta_t) \cdot \mathcal{E}_t(t) \cdot \varepsilon(m_{hh}, \Omega), \quad (5)$$

where $\varepsilon(m_{hh}, \Omega)$ is the efficiency as a function of $\pi^+\pi^-$ mass and angles, obtained from the simulation as described in Ref. [10], $T(t-\hat{t}|\delta_t)$ is the decay time resolution function which depends upon the estimated decay time error for each event δ_t, and $\mathcal{E}_t(t)$ is the decay time acceptance function. The latter two are discussed in Section 5.

The distribution of the background decay time, $\pi^+\pi^-$ mass and angles can be factorized into components for the decay time and the remaining variables. The background decay time distribution, $F_t^{bkg}(t|\delta_t)$ is a double exponential function convolved with the decay time resolution function, taken to be the same as that of the signal, and multiplied by the background decay time acceptance function. The parameters of the double exponential function and the acceptance function are obtained from the sum of $J/\psi\pi^+\pi^+$ and $J/\psi\pi^-\pi^-$ combinations in the same mass signal window as the $J/\psi\pi^+\pi^-$. The distribution of the background for the $\pi^+\pi^-$ mass and angles is described by the function $B^{bkg}(m_{hh}, \Omega)$, discussed in Ref. [10], by summing all the backgrounds components.

The events are divided into four tagging categories: tagged by both OS and SSK, by OS only, by SSK only, and untagged. Each category i is described by the PDF

$$P^i(m, t, m_{hh}, \Omega, \eta, \mathfrak{q}, \delta_t) = \frac{(1-f^i_{bkg})}{\mathcal{N}^i_{sig}} P^{sig}_m(m) F^{sig}(t, m_{hh}, \Omega, \mathfrak{q}|\eta, \delta_t) P^{sig}_{\delta_t}(\delta_t) P^{sig}_{\eta,i}(\eta) + \frac{f^i_{bkg}}{\mathcal{N}^i_{bkg}} P^{bkg}_m(m) B^{bkg}(m_{hh}, \Omega) F^{bkg}_t(t|\delta_t) P^{bkg}_{\delta_t}(\delta_t) P^{bkg}_{\eta,i}(\eta), \quad (6)$$

where f^i_{bkg} is the background fraction, which is fixed to the value obtained from the $B^{(-)0}_s$ mass fit for each category. The normalization factors $\mathcal{N}^i$ are calculated for each event by integrating over the decay time t, the dihadron invariant mass m_{hh}, and the angles Ω.

We include the PDFs for the estimated per-candidate decay time error δ_t and the wrong-tag probability η. The $P^{sig}_{\delta_t}(\delta_t)$ and $P^{bkg}_{\delta_t}(\delta_t)$ functions are signal and background PDFs of δ_t. The δ_t background PDF is obtained from the distribution of the like-sign events and the δ_t signal PDF is obtained from the distribution of the $B^{(-)0}_s$ candidates after background subtraction. The signal peaks at about 26 fs and the background at 29 fs. The mistagging PDF is different in each of the tagging categories: it is a product of two one-dimensional PDFs of η^{SSK} and η^{OS} if both are tagged, a one-dimensional PDF of the corresponding tagger if only single tagged, and a uniform PDF if untagged. The two one-dimensional distributions of η^{SSK} and η^{OS} are shown in Fig. 3 for both signal and background.

5. Decay time resolution and acceptance

The decay time resolution function $T(t-\hat{t}; \delta t)$ is described by a sum of three Gaussian functions with a common mean, and widths given by three scale factors, each being multiplied by $\sigma_t \equiv \delta_t + \sigma_t^0$, where δ_t is the estimated per-event decay time error and σ_t^0 is a constant parameter. Studies on simulated data show that prompt $J/\psi\pi^+\pi^-$ combinations have nearly identical resolution to signal events. Consequently, we determine the parameters of the resolution model from a fit to the decay time distribution of such prompt combinations in the data, where the contribution of candidates unlikely to originate from J/ψ events are subtracted using sidebands of the $\mu^+\mu^-$ invariant mass distribution away from the J/ψ mass peak. Specifically, the time resolution is determined using prompt J/ψ, triggered specially for calibration purposes, plus two oppositely charged tracks from the primary vertex with similar selection criteria as for $J/\psi\pi^+\pi^-$. We require that the $J/\psi\pi^+\pi^-$ mass be within ± 20 MeV of the $\overline{B}^0_s$ mass, and we do not require the tracks to be detached. Taking into account the δ_t distribution of the $B^{(-)0}_s$ signal, the effective resolution is found to be 40.3 fs by using the weighted average widths of the three Gaussians.

The decay time distribution is influenced by acceptance effects that are introduced by track reconstruction, trigger and event selection. The decay time acceptance is obtained using control samples of $\overline{B}_0 \to J/\psi \overline{K}^{*0}(\to K^-\pi^+)$ and $B^0 \to J/\psi K^{*0}(\to K^+\pi^-)$ decays, and then corrected by the acceptance ratio between $\overline{B}^0_s$ and $\overline{B}_0$ decays derived from the simulation.

The same selection as for signal events is implemented for the $B^{(-)0}$ candidates except for the kaon identification requirement. The $K^\mp\pi^\pm$ pair mass is restricted within ± 100 MeV of the nominal $\overline{K}^{*0}$ mass [28]. The candidates within ± 25 MeV of the $\overline{B}_0$ mass peak are used to measure the decay time acceptance. There are $399\,200 \pm 800$ signal events with a purity of 98.5%. The decay time distribution is shown in Fig. 4(a). These data are fitted with an exponential function convolved with the time resolution function, and then multiplied by the acceptance function, $\frac{[a(t-t_0)]^n}{1+[a(t-t_0)]^n} \times (1 + \beta t + \beta_2 t^2)$, where a, n, t_0, β, and β_2 are parameters determined by the fit. The $\overline{B}_0$ lifetime is constrained to

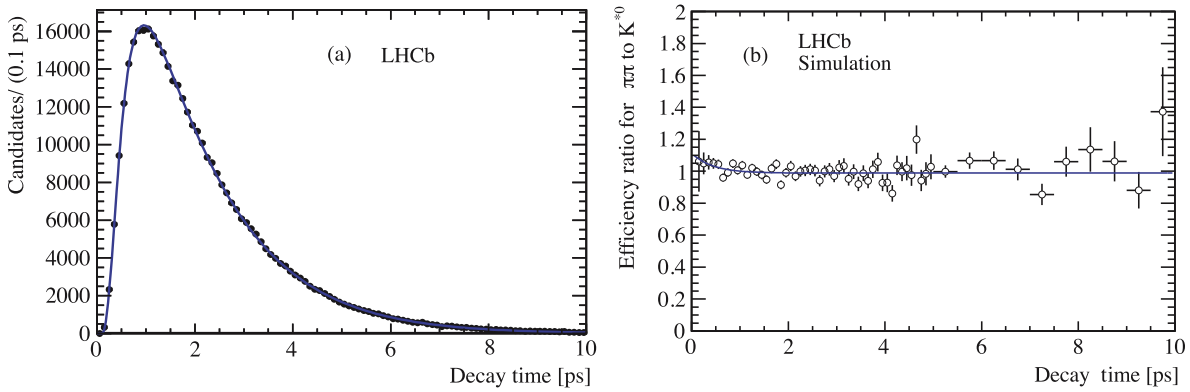

Fig. 4. Distributions of (a) decay time of $\overline{(-)}{B}^0 \to J/\psi \overline{(-)}{K}^{*0}$ candidates in data, (b) ratio of time acceptance between $\overline{(-)}{B}^0_s \to J/\psi\pi^+\pi^-$ and $\overline{(-)}{B}^0 \to J/\psi \overline{(-)}{K}^{*0}$ decays from simulation.

Table 1
Acceptance function parameter values and their correlations.

	Parameter correlations							Values
	n	a	β	β_2	t_0	p_1	p_2	
n	1.00	0.44	0.57	−0.54	−0.86	0.00	0.00	2.082 ± 0.036
a	0.44	1.00	0.74	−0.74	−0.05	0.00	0.00	1.981 ± 0.024 ps^{-1}
β	0.57	0.74	1.00	−0.90	−0.37	0.00	0.00	0.077 ± 0.009 ps^{-1}
β_2	−0.54	−0.74	−0.90	1.00	0.34	0.00	0.00	-0.008 ± 0.001 ps^{-2}
t_0	−0.86	−0.05	−0.37	0.34	1.00	0.00	0.00	0.104 ± 0.003 ps
p_1	0.00	0.00	0.00	0.00	0.00	1.00	−0.89	2.290 ± 1.761 ps^{-1}
p_2	0.00	0.00	0.00	0.00	0.00	−0.89	1.00	-0.124 ± 0.110

$\tau_{B^0} = 1.519 \pm 0.007$ ps [28]. The signal acceptance parameters and their correlations are given in Table 1. There is a large efficiency drop below 1 ps due to detachment requirements on the $\overline{(-)}{B}^0$ and its decay products in the selection.

Fig. 4(b) shows the acceptance ratio between $\overline{(-)}{B}^0_s \to J/\psi\pi^+\pi^-$ and $\overline{(-)}{B}^0 \to J/\psi \overline{(-)}{K}^{*0}$ decays from the simulation. The distribution is almost flat. The ratio is well described by the function $R(1 - p_2 e^{-p_1 t})$ with parameters R, p_1 and p_2 determined by the fit. Parameter R is a normalization constant.

We use the product of the acceptance determined from $\overline{(-)}{B}^0 \to J/\psi \overline{(-)}{K}^{*0}$ decays and the correction ratio found from simulation as the decay time acceptance function for $\overline{B}^0_s$, denoted as $\mathcal{E}_t(t; a, n, t_0, \beta, \beta_2, p_1, p_2)$, where the parameter values and correlations are given in Table 1.

6. Results

The *CP* phase ϕ_s is determined from the fit that uses the amplitude model with five final state $\pi^+\pi^-$ resonances. Several of the model parameters have Gaussian constraints applied in the fit. They are the measured values of $\Delta m_s = 17.768 \pm 0.024$ ps^{-1} [29], $\Gamma_s = 0.663 \pm 0.005 \pm 0.006$ ps^{-1} and $\Delta\Gamma_s = 0.100 \pm 0.016 \pm 0.003$ ps^{-1} [4], the tagging parameters, the mass and width of the $f_0(1790)$ [30], the $f_2'(1525)$ fit fractions, and the scale factors in the decay time resolution function, multiplied by (1.00 ± 0.05) to take into account the systematic uncertainty on the decay time resolution estimate [5]. Apart from ϕ_s and $|\lambda|$, the other free parameters are the amplitudes and phases of the $\pi^+\pi^-$ states. The fit procedure is checked using pseudoexperiments with the same size as data. The fit reproduces the input ϕ_s values with negligible bias.

For our first fit we do not allow direct *CP* violation and therefore fix $|\lambda|$ to 1. The fit determines $\phi_s = 75 \pm 67 \pm 8$ mrad. When two uncertainties are quoted, the first is statistical and the second the systematic. The systematic uncertainty is discussed in Section 7. Fig. 5 shows the decay time distribution superimposed with the fit projection. Projections for m_{hh} and Ω are shown in Fig. 2. Fit fractions of the contributing resonances are consistent with the results from the amplitude analysis [10]. We also perform the fit with $|\lambda|$ treated as a free parameter. The fit determines $\phi_s = 70 \pm 68 \pm 8$ mrad and $|\lambda| = 0.89 \pm 0.05 \pm 0.01$, consistent with no direct *CP* violation ($|\lambda| = 1$), under the assumption that direct *CP* violation is equal for all of the intermediate $\pi^+\pi^-$ states. (The correlation between ϕ_s and $|\lambda|$ is about 1%.)

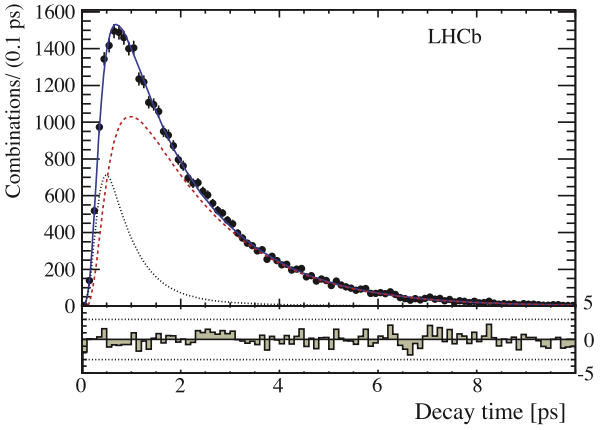

Fig. 5. Decay time distribution of $\overline{(-)}{B}^0_s \to J/\psi\pi^+\pi^-$ candidates. The signal PDF is shown with a (red) dashed line, the background with a (black) dotted line, and the (blue) solid line represents the total. (The reader is referred to the web version of this article to see the figure in color.)

Since the $J/\psi\pi^+\pi^-$ final state is known to be >97.7% CP-odd at 95% CL [10], we check our result by implementing a simplified fit without using the information of m_{hh} and Ω. Here the *CP*-odd fraction is assumed to be 100%, thus angular information is not needed to separate *CP*-odd and possible *CP*-even components. This fit was used in the previous ϕ_s measurement using $J/\psi\pi^+\pi^-$ de-

Table 2
Systematic uncertainties. The total is the sum in quadrature of each entry.

Sources	ϕ_s (mrad)	λ
Decay time acceptance	±0.6	±0.0008
Mass acceptance	±0.3	±0.0003
Background time PDF	±0.2	±0.0011
Background mass distribution PDF	±0.6	±0.0016
Resonance model	±6.0	±0.0100
Resonance parameters	±0.7	±0.0007
Other fixed parameters	±0.4	±0.0009
Production asymmetry	±5.8	±0.0017
Total	±8.4	±0.010

cays [5]. Compared to the fit discussed above, the simplified fit gives a ϕ_s value differing by 20 mrad and a statistical uncertainty of ±69 mrad. The small difference between the two fits is consistent with a study using pseudoexperiments, where the distribution of the difference between the two fits is a Gaussian with a mean of zero and a width of 20 mrad.

7. Systematic uncertainties

The systematic uncertainties on ϕ_s and $|\lambda|$, evaluated using the fit allowing direct *CP*-violation, are summarized in Table 2. They are small compared to the statistical uncertainty. Since Gaussian constraints are applied in the fit, no additional uncertainty is introduced by the input parameters Δm_s, Γ_s, $\Delta\Gamma_s$, or those associated with flavour tagging and time resolution.

To evaluate the uncertainties due to the fixed parameters in the decay time acceptance, background decay time PDF, $m(\pi^+\pi^-)$ and $m(J/\psi\pi^\pm)$ (mass) acceptance and background mass PDF, the data fit is repeated by varying the fixed parameters from their nominal values according to the error matrix 200 times for each source. The matrix elements are determined using simulation, $J/\psi\overline{K}^*$ data, and like-sign dipion data. The r.m.s. of the fitted ϕ_s value is taken as the uncertainty for each source.

Including different resonances could change the *CP*-even fraction in the decay, and thus the ϕ_s result. In Ref. [10] two acceptable solutions were found for the contributing components. For our main result we use the one with five resonant components. The other solution adds a 5.9% nonresonant component. Evaluating ϕ_s for the second solution gives a small difference of 3 mrad. Adding a $\rho(770)$ component causes the largest change for ϕ_s and λ and is taken as the systematic uncertainty, even though vector particles must conserve the zero isospin of the dipion system, which forbids the decay into $\rho(770)$. The resonance masses and widths of $f_2(1270)$ and $f_2'(1525)$ are fixed in the fit.

To evaluate the uncertainty due to the fixed masses and widths, the fit is repeated by changing each parameter within one standard deviation of its error, and the larger shift in the fitted values is taken as the systematic uncertainty. Similarly, the uncertainties due to other fixed parameters, such as background fractions and those used in $\overset{(-)}{B}$ mass PDFs, are also determined. We take the background decay time distribution to be independent of m_{hh}. This assumption is tested by repeating the fit with different background decay time PDFs for the low m_{hh} and high m_{hh} regions, found from the like-sign dipion events in the same mass regions. The effects on ϕ_s and $|\lambda|$ are found to be negligible.

The production ratio of $\overline{B}{}_s^0$ to B_s^0 is estimated to be $R_P = (1.00 \pm 0.05)$ [31]. To include this effect, the $\overline{B}{}_s^0$ decay rate, $\bar{\Gamma}$, used in Eq. (4) is multiplied by R_P. The uncertainty due to this source is estimated by varying R_P within its error. The uncertainties are added in quadrature to give the total.

8. Conclusions

We have presented a time-dependent flavour-tagged analysis of the $\overset{(-)}{B}{}_s^0 \to J/\psi\pi^+\pi^-$ decay using angular distributions and the $\pi^+\pi^-$ mass dependence to determine the *CP* content of the final state components. We measure the mixing induced *CP*-violating phase ϕ_s. Assuming the absence of direct *CP* violation, we find

$$\phi_s = 75 \pm 67 \pm 8 \text{ mrad}.$$

For the case where direct *CP* is allowed, we find

$$\phi_s = 70 \pm 68 \pm 8 \text{ mrad}, \quad \text{and} \quad |\lambda| = 0.89 \pm 0.05 \pm 0.01.$$

This result supersedes and is more precise than our previous measurement in this decay mode of $\phi_s = -19^{+173+4}_{-174-3}$ mrad based on a 1 fb^{-1} data sample [5]. Physics beyond the Standard Model is not established by our measurements.

Acknowledgements

We express our gratitude to our colleagues in the CERN accelerator departments for the excellent performance of the LHC. We thank the technical and administrative staff at the LHCb institutes. We acknowledge support from CERN and from the national agencies: CAPES, CNPq, FAPERJ and FINEP (Brazil); NSFC (China); CNRS/IN2P3 and Region Auvergne (France); BMBF, DFG, HGF and MPG (Germany); SFI (Ireland); INFN (Italy); FOM and NWO (The Netherlands); SCSR (Poland); MEN/IFA (Romania); MinES, Rosatom, RFBR and NRC "Kurchatov Institute" (Russia); MinECo, XuntaGal and GENCAT (Spain); SNSF and SER (Switzerland); NASU (Ukraine); STFC and the Royal Society (United Kingdom); NSF (USA). We also acknowledge the support received from EPLANET, Marie Curie Actions and the ERC under FP7. The Tier1 computing centres are supported by IN2P3 (France), KIT and BMBF (Germany), INFN (Italy), NWO and SURF (The Netherlands), PIC (Spain), GridPP (United Kingdom). We are indebted to the communities behind the multiple open source software packages on which we depend. We are also thankful for the computing resources and the access to software R&D tools provided by Yandex LLC (Russia).

References

[1] I. Dunietz, R. Fleischer, U. Nierste, In pursuit of new physics with B_s decays, Phys. Rev. D 63 (2001) 114015, arXiv:hep-ph/0012219.
[2] J. Charles, et al., Predictions of selected flavour observables within the Standard Model, Phys. Rev. D 84 (2011) 033005, arXiv:1106.4041.
[3] CDF Collaboration, T. Aaltonen, et al., First flavor-tagged determination of bounds on mixing-induced CP violation in $B_s^0 \to J/\psi\phi$ decays, Phys. Rev. Lett. 100 (2008) 161802, arXiv:0712.2397;
D0 Collaboration, V. Abazov, et al., Measurement of B_s^0 mixing parameters from the flavor-tagged decay $B_s^0 \to J/\psi\phi$, Phys. Rev. Lett. 101 (2008) 241801, arXiv:0802.2255;
CDF Collaboration, T. Aaltonen, et al., Measurement of the CP-violating phase β_s in $B_s^0 \to J/\psi\phi$ decays with the CDF II detector, Phys. Rev. D 85 (2012) 072002, arXiv:1112.1726;
D0 Collaboration, V.M. Abazov, et al., Measurement of the *CP*-violating phase $\phi_s^{J/\psi\phi}$ using the flavor-tagged decay $B_s^0 \to J/\psi\phi$ in 8 fb^{-1} of $p\bar{p}$ collisions, Phys. Rev. D 85 (2012) 032006, arXiv:1109.3166.
[4] LHCb Collaboration, R. Aaij, et al., Measurement of *CP* violation and the B_s^0 meson decay width difference with $B_s^0 \to J/\psi K^+K^-$ and $B_s^0 \to J/\psi\pi^+\pi^-$ decays, Phys. Rev. D 87 (2013) 112010, arXiv:1304.2600.
[5] LHCb Collaboration, R. Aaij, et al., Measurement of the CP-violating phase ϕ_s in $\overline{B}{}_s^0 \to J/\psi\pi^+\pi^-$ decays, Phys. Lett. B 713 (2012) 378, arXiv:1204.5675.
[6] CDF Collaboration, T. Aaltonen, et al., Measurement of the bottom-strange meson mixing phase in the full CDF data set, Phys. Rev. Lett. 109 (2012) 171802, arXiv:1208.2967.
[7] ATLAS Collaboration, G. Aad, et al., Time-dependent angular analysis of the decay $B_s^0 \to J/\psi\phi$ and extraction of $\Delta\Gamma_s$ and the CP-violating weak phase ϕ_s by ATLAS, JHEP 12 (2012) 072, arXiv:1208.0572.

[8] LHCb Collaboration, R. Aaij, et al., Analysis of the resonant components in $\overline{B}{}^0_s \to J/\psi\pi^+\pi^-$, Phys. Rev. D 86 (2012) 052006, arXiv:1204.5643.
[9] L. Zhang, S. Stone, Time-dependent Dalitz-plot formalism for $B^0_q \to J/\psi h^+h^-$, Phys. Lett. B 719 (2013) 383, arXiv:1212.6434.
[10] LHCb Collaboration, R. Aaij, et al., Measurement of resonant and *CP* components in $\overline{B}{}^0_s \to J/\psi\pi^+\pi^-$ decays, Phys. Rev. D 89 (2014) 092006, arXiv:1402.6248.
[11] S. Stone, L. Zhang, S-waves and the measurement of CP violating phases in B_s decays, Phys. Rev. D 79 (2009) 074024, arXiv:0812.2832.
[12] R. Fleischer, R. Knegjens, G. Ricciardi, Anatomy of $B^0_{s,d} \to J/\psi f_0(980)$, Eur. Phys. J. C 71 (2011) 1832, arXiv:1109.1112.
[13] LHCb Collaboration, R. Aaij, et al., Measurement of the resonant and CP components in $\overline{B}{}^0 \to J/\psi\pi^+\pi^-$ decays, Phys. Rev. D (2015), in press, arXiv:1404.5673.
[14] S. Stone, L. Zhang, Use of $B \to J/\psi f_0$ decays to discern the $q\bar{q}$ or tetraquark nature of scalar mesons, Phys. Rev. Lett. 111 (6) (2013) 062001, arXiv:1305.6554.
[15] U. Nierste, Three lectures on meson mixing and CKM phenomenology, arXiv:0904.1869;
I.I. Bigi, A. Sanda, CP violation, Camb. Monogr. Part. Phys. Nucl. Phys. Cosmol. 9 (2000) 1.
[16] A.S. Dighe, I. Dunietz, H.J. Lipkin, J.L. Rosner, Angular distributions and lifetime differences in $B^0_s \to J/\psi\phi$ decays, Phys. Lett. B 369 (1996) 144, arXiv:hep-ph/9511363.
[17] LHCb Collaboration, R. Aaij, et al., Measurement of the flavour-specific CP-violating asymmetry a^s_{sl} in B^0_s decays, Phys. Lett. B 728 (2014) 607, arXiv:1308.1048.
[18] LHCb Collaboration, A. Alves Jr., et al., The LHCb detector at the LHC, J. Instrum. 3 (2008) S08005.
[19] T. Sjöstrand, S. Mrenna, P. Skands, PYTHIA 6.4 physics and manual, JHEP 605 (2006) 026, arXiv:hep-ph/0603175;
T. Sjöstrand, S. Mrenna, P. Skands, A brief introduction to PYTHIA 8.1, Comput. Phys. Commun. 178 (2008) 852, arXiv:0710.3820.
[20] I. Belyaev, et al., Handling of the generation of primary events in Gauss, the LHCb simulation framework, Nuclear Science Symposium Conference Record (NSS/MIC) IEEE (2010) 1155.
[21] D.J. Lange, The EvtGen particle decay simulation package, Nucl. Instrum. Methods Phys. Res., Sect. A, Accel. Spectrom. Detect. Assoc. Equip. 462 (2001) 152.
[22] P. Golonka, Z. Was, PHOTOS Monte, Carlo: a precision tool for QED corrections in Z and W decays, Eur. Phys. J. C 45 (2006) 97, arXiv:hep-ph/0506026.
[23] Geant4 Collaboration, J. Allison, et al., Geant4 developments and applications, IEEE Trans. Nucl. Sci. 53 (2006) 270;
GEANT4 Collaboration, S. Agostinelli, et al., GEANT4: a simulation toolkit, Nucl. Instrum. Methods Phys. Res., Sect. A, Accel. Spectrom. Detect. Assoc. Equip. 506 (2003) 250.
[24] M. Clemencic, et al., The LHCb simulation application, Gauss: design, evolution and experience, J. Phys. Conf. Ser. 331 (2011) 032023.
[25] T. Skwarnicki, A study of the radiative cascade transitions between the Upsilon-prime and Upsilon resonances, PhD thesis, Institute of Nuclear Physics, Krakow, 1986, DESY-F31-86-02.
[26] LHCb Collaboration, R. Aaij, et al., Opposite-side flavour tagging of B mesons at the LHCb experiment, Eur. Phys. J. C 72 (2012) 2022, arXiv:1202.4979.
[27] G.A. Krocker, Development and calibration of a same side kaon tagging algorithm and measurement of the B^0_s–$\overline{B}{}^0_s$ oscillation frequency Δm_s at the LHCb experiment, PhD thesis, Heidelberg University, 2013, CERN-THESIS-2013-213.
[28] Particle Data Group, J. Beringer, et al., Review of particle physics, Phys. Rev. D 86 (2012) 010001, and 2013 update for 2014.
[29] LHCb Collaboration, R. Aaij, et al., Precision measurement of the B^0_s-$\bar{B}^0_s$ oscillation frequency with the decay $B^0_s \to D^-_s\pi^+$, New J. Phys. 15 (2013) 053021, arXiv:1304.4741.
[30] BES Collaboration, M. Ablikim, et al., Resonances in $J/\psi \to \phi\pi^+\pi^-$ and ϕK^+K^-, Phys. Lett. B 607 (2005) 243, arXiv:hep-ex/0411001.
[31] E. Norrbin, R. Vogt, Bottom production asymmetries at the LHC, arXiv:hep-ph/0003056, in: Proceedings of the CERN 1999 Workshop on SM Physics (and more) at the LHC.

LHCb Collaboration

R. Aaij [41], B. Adeva [37], M. Adinolfi [46], A. Affolder [52], Z. Ajaltouni [5], S. Akar [6], J. Albrecht [9], F. Alessio [38], M. Alexander [51], S. Ali [41], G. Alkhazov [30], P. Alvarez Cartelle [37], A.A. Alves Jr. [25,38], S. Amato [2], S. Amerio [22], Y. Amhis [7], L. An [3], L. Anderlini [17,g], J. Anderson [40], R. Andreassen [57], M. Andreotti [16,f], J.E. Andrews [58], R.B. Appleby [54], O. Aquines Gutierrez [10], F. Archilli [38], A. Artamonov [35], M. Artuso [59], E. Aslanides [6], G. Auriemma [25,n], M. Baalouch [5], S. Bachmann [11], J.J. Back [48], A. Badalov [36], V. Balagura [31], W. Baldini [16], R.J. Barlow [54], C. Barschel [38], S. Barsuk [7], W. Barter [47], V. Batozskaya [28], V. Battista [39], A. Bay [39], L. Beaucourt [4], J. Beddow [51], F. Bedeschi [23], I. Bediaga [1], S. Belogurov [31], K. Belous [35], I. Belyaev [31], E. Ben-Haim [8], G. Bencivenni [18], S. Benson [38], J. Benton [46], A. Berezhnoy [32], R. Bernet [40], M.-O. Bettler [47], M. van Beuzekom [41], A. Bien [11], S. Bifani [45], T. Bird [54], A. Bizzeti [17,i], P.M. Bjørnstad [54], T. Blake [48], F. Blanc [39], J. Blouw [10], S. Blusk [59], V. Bocci [25], A. Bondar [34], N. Bondar [30,38], W. Bonivento [15,38], S. Borghi [54], A. Borgia [59], M. Borsato [7], T.J.V. Bowcock [52], E. Bowen [40], C. Bozzi [16], T. Brambach [9], J. van den Brand [42], J. Bressieux [39], D. Brett [54], M. Britsch [10], T. Britton [59], J. Brodzicka [54], N.H. Brook [46], H. Brown [52], A. Bursche [40], G. Busetto [22,r], J. Buytaert [38], S. Cadeddu [15], R. Calabrese [16,f], M. Calvi [20,k], M. Calvo Gomez [36,p], A. Camboni [36], P. Campana [18,38], D. Campora Perez [38], A. Carbone [14,d], G. Carboni [24,l], R. Cardinale [19,38,j], A. Cardini [15], H. Carranza-Mejia [50], L. Carson [50], K. Carvalho Akiba [2], G. Casse [52], L. Cassina [20], L. Castillo Garcia [38], M. Cattaneo [38], Ch. Cauet [9], R. Cenci [58], M. Charles [8], Ph. Charpentier [38], S. Chen [54], S.-F. Cheung [55], N. Chiapolini [40], M. Chrzaszcz [40,26], K. Ciba [38], X. Cid Vidal [38], G. Ciezarek [53], P.E.L. Clarke [50], M. Clemencic [38], H.V. Cliff [47], J. Closier [38], V. Coco [38], J. Cogan [6], E. Cogneras [5], P. Collins [38], A. Comerma-Montells [11], A. Contu [15], A. Cook [46], M. Coombes [46], S. Coquereau [8], G. Corti [38], M. Corvo [16,f], I. Counts [56], B. Couturier [38], G.A. Cowan [50], D.C. Craik [48], M. Cruz Torres [60], S. Cunliffe [53], R. Currie [50], C. D'Ambrosio [38], J. Dalseno [46], P. David [8], P.N.Y. David [41], A. Davis [57], K. De Bruyn [41], S. De Capua [54], M. De Cian [11], J.M. De Miranda [1], L. De Paula [2], W. De Silva [57], P. De Simone [18], D. Decamp [4], M. Deckenhoff [9], L. Del Buono [8], N. Déléage [4], D. Derkach [55], O. Deschamps [5], F. Dettori [42], A. Di Canto [38], H. Dijkstra [38], S. Donleavy [52], F. Dordei [11], M. Dorigo [39], A. Dosil Suárez [37], D. Dossett [48], A. Dovbnya [43], K. Dreimanis [52], G. Dujany [54], F. Dupertuis [39], P. Durante [38], R. Dzhelyadin [35], A. Dziurda [26], A. Dzyuba [30], S. Easo [49,38], U. Egede [53], V. Egorychev [31], S. Eidelman [34], S. Eisenhardt [50], U. Eitschberger [9], R. Ekelhof [9], L. Eklund [51,38], I. El Rifai [5], Ch. Elsasser [40],

S. Ely [59], S. Esen [11], T. Evans [55], A. Falabella [16,f], C. Färber [11], C. Farinelli [41], N. Farley [45], S. Farry [52], D. Ferguson [50], V. Fernandez Albor [37], F. Ferreira Rodrigues [1], M. Ferro-Luzzi [38], S. Filippov [33], M. Fiore [16,f], M. Fiorini [16,f], M. Firlej [27], C. Fitzpatrick [38], T. Fiutowski [27], M. Fontana [10], F. Fontanelli [19,j], R. Forty [38], O. Francisco [2], M. Frank [38], C. Frei [38], M. Frosini [17,38,g], J. Fu [21,38], E. Furfaro [24,l], A. Gallas Torreira [37], D. Galli [14,d], S. Gallorini [22], S. Gambetta [19,j], M. Gandelman [2], P. Gandini [59], Y. Gao [3], J. Garofoli [59], J. Garra Tico [47], L. Garrido [36], C. Gaspar [38], R. Gauld [55], L. Gavardi [9], G. Gavrilov [30], E. Gersabeck [11], M. Gersabeck [54], T. Gershon [48], Ph. Ghez [4], A. Gianelle [22], S. Giani' [39], V. Gibson [47], L. Giubega [29], V.V. Gligorov [38], C. Göbel [60], D. Golubkov [31], A. Golutvin [53,31,38], A. Gomes [1,a], H. Gordon [38], C. Gotti [20], M. Grabalosa Gándara [5], R. Graciani Diaz [36], L.A. Granado Cardoso [38], E. Graugés [36], G. Graziani [17], A. Grecu [29], E. Greening [55], S. Gregson [47], P. Griffith [45], L. Grillo [11], O. Grünberg [62], B. Gui [59], E. Gushchin [33], Yu. Guz [35,38], T. Gys [38], C. Hadjivasiliou [59], G. Haefeli [39], C. Haen [38], S.C. Haines [47], S. Hall [53], B. Hamilton [58], T. Hampson [46], X. Han [11], S. Hansmann-Menzemer [11], N. Harnew [55], S.T. Harnew [46], J. Harrison [54], T. Hartmann [62], J. He [38], T. Head [38], V. Heijne [41], K. Hennessy [52], P. Henrard [5], L. Henry [8], J.A. Hernando Morata [37], E. van Herwijnen [38], M. Heß [62], A. Hicheur [1], D. Hill [55], M. Hoballah [5], C. Hombach [54], W. Hulsbergen [41], P. Hunt [55], N. Hussain [55], D. Hutchcroft [52], D. Hynds [51], M. Idzik [27], P. Ilten [56], R. Jacobsson [38], A. Jaeger [11], J. Jalocha [55], E. Jans [41], P. Jaton [39], A. Jawahery [58], F. Jing [3], M. John [55], D. Johnson [55], C.R. Jones [47], C. Joram [38], B. Jost [38], N. Jurik [59], M. Kaballo [9], S. Kandybei [43], W. Kanso [6], M. Karacson [38], T.M. Karbach [38], S. Karodia [51], M. Kelsey [59], I.R. Kenyon [45], T. Ketel [42], B. Khanji [20], C. Khurewathanakul [39], S. Klaver [54], O. Kochebina [7], M. Kolpin [11], I. Komarov [39], R.F. Koopman [42], P. Koppenburg [41,38], M. Korolev [32], A. Kozlinskiy [41], L. Kravchuk [33], K. Kreplin [11], M. Kreps [48], G. Krocker [11], P. Krokovny [34], F. Kruse [9], W. Kucewicz [26,o], M. Kucharczyk [20,26,38,k], V. Kudryavtsev [34], K. Kurek [28], T. Kvaratskheliya [31], V.N. La Thi [39], D. Lacarrere [38], G. Lafferty [54], A. Lai [15], D. Lambert [50], R.W. Lambert [42], E. Lanciotti [38], G. Lanfranchi [18], C. Langenbruch [38], B. Langhans [38], T. Latham [48], C. Lazzeroni [45], R. Le Gac [6], J. van Leerdam [41], J.-P. Lees [4], R. Lefèvre [5], A. Leflat [32], J. Lefrançois [7], S. Leo [23], O. Leroy [6], T. Lesiak [26], B. Leverington [11], Y. Li [3], M. Liles [52], R. Lindner [38], C. Linn [38], F. Lionetto [40], B. Liu [15], G. Liu [38], S. Lohn [38], I. Longstaff [51], J.H. Lopes [2], N. Lopez-March [39], P. Lowdon [40], H. Lu [3], D. Lucchesi [22,r], H. Luo [50], A. Lupato [22], E. Luppi [16,f], O. Lupton [55], F. Machefert [7], I.V. Machikhiliyan [31], F. Maciuc [29], O. Maev [30], S. Malde [55], G. Manca [15,e], G. Mancinelli [6], J. Maratas [5], J.F. Marchand [4], U. Marconi [14], C. Marin Benito [36], P. Marino [23,t], R. Märki [39], J. Marks [11], G. Martellotti [25], A. Martens [8], A. Martín Sánchez [7], M. Martinelli [41], D. Martinez Santos [42], F. Martinez Vidal [64], D. Martins Tostes [2], A. Massafferri [1], R. Matev [38], Z. Mathe [38], C. Matteuzzi [20], A. Mazurov [16,f], M. McCann [53], J. McCarthy [45], A. McNab [54], R. McNulty [12], B. McSkelly [52], B. Meadows [57], F. Meier [9], M. Meissner [11], M. Merk [41], D.A. Milanes [8], M.-N. Minard [4], N. Moggi [14], J. Molina Rodriguez [60], S. Monteil [5], M. Morandin [22], P. Morawski [27], A. Mordà [6], M.J. Morello [23,t], J. Moron [27], A.-B. Morris [50], R. Mountain [59], F. Muheim [50], K. Müller [40], R. Muresan [29], M. Mussini [14], B. Muster [39], P. Naik [46], T. Nakada [39], R. Nandakumar [49], I. Nasteva [2], M. Needham [50], N. Neri [21], S. Neubert [38], N. Neufeld [38], M. Neuner [11], A.D. Nguyen [39], T.D. Nguyen [39], C. Nguyen-Mau [39,q], M. Nicol [7], V. Niess [5], R. Niet [9], N. Nikitin [32], T. Nikodem [11], A. Novoselov [35], D.P. O'Hanlon [48], A. Oblakowska-Mucha [27], V. Obraztsov [35], S. Oggero [41], S. Ogilvy [51], O. Okhrimenko [44], R. Oldeman [15,e], G. Onderwater [65], M. Orlandea [29], J.M. Otalora Goicochea [2], P. Owen [53], A. Oyanguren [64], B.K. Pal [59], A. Palano [13,c], F. Palombo [21,u], M. Palutan [18], J. Panman [38], A. Papanestis [49,38], M. Pappagallo [51], C. Parkes [54], C.J. Parkinson [9], G. Passaleva [17], G.D. Patel [52], M. Patel [53], C. Patrignani [19,j], A. Pazos Alvarez [37], A. Pearce [54], A. Pellegrino [41], M. Pepe Altarelli [38], S. Perazzini [14,d], E. Perez Trigo [37], P. Perret [5], M. Perrin-Terrin [6], L. Pescatore [45], E. Pesen [66], K. Petridis [53], A. Petrolini [19,j], E. Picatoste Olloqui [36], B. Pietrzyk [4], T. Pilař [48], D. Pinci [25], A. Pistone [19], S. Playfer [50], M. Plo Casasus [37], F. Polci [8], A. Poluektov [48,34], E. Polycarpo [2], A. Popov [35], D. Popov [10], B. Popovici [29], C. Potterat [2], J. Prisciandaro [39], A. Pritchard [52], C. Prouve [46], V. Pugatch [44], A. Puig Navarro [39], G. Punzi [23,s], W. Qian [4], B. Rachwal [26], J.H. Rademacker [46], B. Rakotomiaramanana [39], M. Rama [18], M.S. Rangel [2], I. Raniuk [43], N. Rauschmayr [38], G. Raven [42], S. Reichert [54], M.M. Reid [48], A.C. dos Reis [1], S. Ricciardi [49], A. Richards [53], M. Rihl [38], K. Rinnert [52], V. Rives Molina [36], D.A. Roa Romero [5], P. Robbe [7], A.B. Rodrigues [1], E. Rodrigues [54], P. Rodriguez Perez [54], S. Roiser [38], V. Romanovsky [35], A. Romero Vidal [37], M. Rotondo [22], J. Rouvinet [39], T. Ruf [38], F. Ruffini [23], H. Ruiz [36], P. Ruiz Valls [64], G. Sabatino [25,l], J.J. Saborido Silva [37], N. Sagidova [30], P. Sail [51], B. Saitta [15,e],

V. Salustino Guimaraes [2], C. Sanchez Mayordomo [64], B. Sanmartin Sedes [37], R. Santacesaria [25], C. Santamarina Rios [37], E. Santovetti [24,l], M. Sapunov [6], A. Sarti [18,m], C. Satriano [25,n], A. Satta [24], M. Savrie [16,f], D. Savrina [31,32], M. Schiller [42], H. Schindler [38], M. Schlupp [9], M. Schmelling [10], B. Schmidt [38], O. Schneider [39], A. Schopper [38], M.-H. Schune [7], R. Schwemmer [38], B. Sciascia [18], A. Sciubba [25], M. Seco [37], A. Semennikov [31], I. Sepp [53], N. Serra [40], J. Serrano [6], L. Sestini [22], P. Seyfert [11], M. Shapkin [35], I. Shapoval [16,43,f], Y. Shcheglov [30], T. Shears [52], L. Shekhtman [34], V. Shevchenko [63], A. Shires [9], R. Silva Coutinho [48], G. Simi [22], M. Sirendi [47], N. Skidmore [46], T. Skwarnicki [59], N.A. Smith [52], E. Smith [55,49], E. Smith [53], J. Smith [47], M. Smith [54], H. Snoek [41], M.D. Sokoloff [57], F.J.P. Soler [51], F. Soomro [39], D. Souza [46], B. Souza De Paula [2], B. Spaan [9], A. Sparkes [50], P. Spradlin [51], F. Stagni [38], M. Stahl [11], S. Stahl [11], O. Steinkamp [40], O. Stenyakin [35], S. Stevenson [55], S. Stoica [29], S. Stone [59,*], B. Storaci [40], S. Stracka [23,38], M. Straticiuc [29], U. Straumann [40], R. Stroili [22], V.K. Subbiah [38], L. Sun [57], W. Sutcliffe [53], K. Swientek [27], S. Swientek [9], V. Syropoulos [42], M. Szczekowski [28], P. Szczypka [39,38], D. Szilard [2], T. Szumlak [27], S. T'Jampens [4], M. Teklishyn [7], G. Tellarini [16,f], F. Teubert [38], C. Thomas [55], E. Thomas [38], J. van Tilburg [41], V. Tisserand [4], M. Tobin [39], S. Tolk [42], L. Tomassetti [16,f], D. Tonelli [38], S. Topp-Joergensen [55], N. Torr [55], E. Tournefier [4], S. Tourneur [39], M.T. Tran [39], M. Tresch [40], A. Tsaregorodtsev [6], P. Tsopelas [41], N. Tuning [41], M. Ubeda Garcia [38], A. Ukleja [28], A. Ustyuzhanin [63], U. Uwer [11], V. Vagnoni [14], G. Valenti [14], A. Vallier [7], R. Vazquez Gomez [18], P. Vazquez Regueiro [37], C. Vázquez Sierra [37], S. Vecchi [16], J.J. Velthuis [46], M. Veltri [17,h], G. Veneziano [39], M. Vesterinen [11], B. Viaud [7], D. Vieira [2], M. Vieites Diaz [37], X. Vilasis-Cardona [36,p], A. Vollhardt [40], D. Volyanskyy [10], D. Voong [46], A. Vorobyev [30], V. Vorobyev [34], C. Voß [62], H. Voss [10], J.A. de Vries [41], R. Waldi [62], C. Wallace [48], R. Wallace [12], J. Walsh [23], S. Wandernoth [11], J. Wang [59], D.R. Ward [47], N.K. Watson [45], D. Websdale [53], M. Whitehead [48], J. Wicht [38], D. Wiedner [11], G. Wilkinson [55], M.P. Williams [45], M. Williams [56], F.F. Wilson [49], J. Wimberley [58], J. Wishahi [9], W. Wislicki [28], M. Witek [26], G. Wormser [7], S.A. Wotton [47], S. Wright [47], S. Wu [3], K. Wyllie [38], Y. Xie [61], Z. Xing [59], Z. Xu [39], Z. Yang [3], X. Yuan [3], O. Yushchenko [35], M. Zangoli [14], M. Zavertyaev [10,b], L. Zhang [59], W.C. Zhang [12], Y. Zhang [3], A. Zhelezov [11], A. Zhokhov [31], L. Zhong [3], A. Zvyagin [38]

[1] *Centro Brasileiro de Pesquisas Físicas (CBPF), Rio de Janeiro, Brazil*
[2] *Universidade Federal do Rio de Janeiro (UFRJ), Rio de Janeiro, Brazil*
[3] *Center for High Energy Physics, Tsinghua University, Beijing, China*
[4] *LAPP, Université de Savoie, CNRS/IN2P3, Annecy-Le-Vieux, France*
[5] *Clermont Université, Université Blaise Pascal, CNRS/IN2P3, LPC, Clermont-Ferrand, France*
[6] *CPPM, Aix-Marseille Université, CNRS/IN2P3, Marseille, France*
[7] *LAL, Université Paris-Sud, CNRS/IN2P3, Orsay, France*
[8] *LPNHE, Université Pierre et Marie Curie, Université Paris Diderot, CNRS/IN2P3, Paris, France*
[9] *Fakultät Physik, Technische Universität Dortmund, Dortmund, Germany*
[10] *Max-Planck-Institut für Kernphysik (MPIK), Heidelberg, Germany*
[11] *Physikalisches Institut, Ruprecht-Karls-Universität Heidelberg, Heidelberg, Germany*
[12] *School of Physics, University College Dublin, Dublin, Ireland*
[13] *Sezione INFN di Bari, Bari, Italy*
[14] *Sezione INFN di Bologna, Bologna, Italy*
[15] *Sezione INFN di Cagliari, Cagliari, Italy*
[16] *Sezione INFN di Ferrara, Ferrara, Italy*
[17] *Sezione INFN di Firenze, Firenze, Italy*
[18] *Laboratori Nazionali dell'INFN di Frascati, Frascati, Italy*
[19] *Sezione INFN di Genova, Genova, Italy*
[20] *Sezione INFN di Milano Bicocca, Milano, Italy*
[21] *Sezione INFN di Milano, Milano, Italy*
[22] *Sezione INFN di Padova, Padova, Italy*
[23] *Sezione INFN di Pisa, Pisa, Italy*
[24] *Sezione INFN di Roma Tor Vergata, Roma, Italy*
[25] *Sezione INFN di Roma La Sapienza, Roma, Italy*
[26] *Henryk Niewodniczanski Institute of Nuclear Physics Polish Academy of Sciences, Kraków, Poland*
[27] *AGH – University of Science and Technology, Faculty of Physics and Applied Computer Science, Kraków, Poland*
[28] *National Center for Nuclear Research (NCBJ), Warsaw, Poland*
[29] *Horia Hulubei National Institute of Physics and Nuclear Engineering, Bucharest-Magurele, Romania*
[30] *Petersburg Nuclear Physics Institute (PNPI), Gatchina, Russia*
[31] *Institute of Theoretical and Experimental Physics (ITEP), Moscow, Russia*
[32] *Institute of Nuclear Physics, Moscow State University (SINP MSU), Moscow, Russia*
[33] *Institute for Nuclear Research of the Russian Academy of Sciences (INR RAN), Moscow, Russia*
[34] *Budker Institute of Nuclear Physics (SB RAS) and Novosibirsk State University, Novosibirsk, Russia*
[35] *Institute for High Energy Physics (IHEP), Protvino, Russia*
[36] *Universitat de Barcelona, Barcelona, Spain*
[37] *Universidad de Santiago de Compostela, Santiago de Compostela, Spain*
[38] *European Organization for Nuclear Research (CERN), Geneva, Switzerland*
[39] *Ecole Polytechnique Fédérale de Lausanne (EPFL), Lausanne, Switzerland*

[40] Physik-Institut, Universität Zürich, Zürich, Switzerland
[41] Nikhef National Institute for Subatomic Physics, Amsterdam, The Netherlands
[42] Nikhef National Institute for Subatomic Physics and VU University Amsterdam, Amsterdam, The Netherlands
[43] NSC Kharkiv Institute of Physics and Technology (NSC KIPT), Kharkiv, Ukraine
[44] Institute for Nuclear Research of the National Academy of Sciences (KINR), Kyiv, Ukraine
[45] University of Birmingham, Birmingham, United Kingdom
[46] H.H. Wills Physics Laboratory, University of Bristol, Bristol, United Kingdom
[47] Cavendish Laboratory, University of Cambridge, Cambridge, United Kingdom
[48] Department of Physics, University of Warwick, Coventry, United Kingdom
[49] STFC Rutherford Appleton Laboratory, Didcot, United Kingdom
[50] School of Physics and Astronomy, University of Edinburgh, Edinburgh, United Kingdom
[51] School of Physics and Astronomy, University of Glasgow, Glasgow, United Kingdom
[52] Oliver Lodge Laboratory, University of Liverpool, Liverpool, United Kingdom
[53] Imperial College London, London, United Kingdom
[54] School of Physics and Astronomy, University of Manchester, Manchester, United Kingdom
[55] Department of Physics, University of Oxford, Oxford, United Kingdom
[56] Massachusetts Institute of Technology, Cambridge, MA, United States
[57] University of Cincinnati, Cincinnati, OH, United States
[58] University of Maryland, College Park, MD, United States
[59] Syracuse University, Syracuse, NY, United States
[60] Pontifícia Universidade Católica do Rio de Janeiro (PUC-Rio), Rio de Janeiro, Brazil [v]
[61] Institute of Particle Physics, Central China Normal University, Wuhan, Hubei, China [w]
[62] Institut für Physik, Universität Rostock, Rostock, Germany [x]
[63] National Research Centre Kurchatov Institute, Moscow, Russia [y]
[64] Instituto de Fisica Corpuscular (IFIC), Universitat de Valencia-CSIC, Valencia, Spain [z]
[65] KVI – University of Groningen, Groningen, The Netherlands [aa]
[66] Celal Bayar University, Manisa, Turkey [ab]

* Corresponding author.
[a] Universidade Federal do Triângulo Mineiro (UFTM), Uberaba MG, Brazil.
[b] P.N. Lebedev Physical Institute, Russian Academy of Science (LPI RAS), Moscow, Russia.
[c] Università di Bari, Bari, Italy.
[d] Università di Bologna, Bologna, Italy.
[e] Università di Cagliari, Cagliari, Italy.
[f] Università di Ferrara, Ferrara, Italy.
[g] Università di Firenze, Firenze, Italy.
[h] Università di Urbino, Urbino, Italy.
[i] Università di Modena e Reggio Emilia, Modena, Italy.
[j] Università di Genova, Genova, Italy.
[k] Università di Milano Bicocca, Milano, Italy.
[l] Università di Roma Tor Vergata, Roma, Italy.
[m] Università di Roma La Sapienza, Roma, Italy.
[n] Università della Basilicata, Potenza, Italy.
[o] AGH – University of Science and Technology, Faculty of Computer Science, Electronics and Telecommunications, Kraków, Poland.
[p] LIFAELS, La Salle, Universitat Ramon Llull, Barcelona, Spain.
[q] Hanoi University of Science, Hanoi, Viet Nam.
[r] Università di Padova, Padova, Italy.
[s] Università di Pisa, Pisa, Italy.
[t] Scuola Normale Superiore, Pisa, Italy.
[u] Università degli Studi di Milano, Milano, Italy.
[v] Associated to Universidade Federal do Rio de Janeiro (UFRJ), Rio de Janeiro, Brazil.
[w] Associated to Center for High Energy Physics, Tsinghua University, Beijing, China.
[x] Associated to Physikalisches Institut, Ruprecht-Karls-Universität Heidelberg, Heidelberg, Germany.
[y] Associated to Institute of Theoretical and Experimental Physics (ITEP), Moscow, Russia.
[z] Associated to Universitat de Barcelona, Barcelona, Spain
[aa] Associated to Nikhef National Institute for Subatomic Physics, Amsterdam, The Netherlands.
[ab] Associated to European Organization for Nuclear Research (CERN), Geneva, Switzerland.